

Performance of superadiabatic quantum machines

Obinna Abah and Eric Lutz

Department of Physics, Friedrich-Alexander-Universität Erlangen-Nürnberg, D-91058 Erlangen, Germany

We investigate the performance of a quantum thermal machine operating in finite time based on shortcut-to-adiabaticity techniques. We compute efficiency and power for a quantum harmonic Otto engine by taking the energetic cost of the superadiabatic driving explicitly into account. We further derive generic upper bounds on both quantities, valid for any heat engine cycle, using the notion of quantum speed limits for driven systems. We demonstrate that these quantum bounds are tighter than those stemming from the second law of thermodynamics.

PACS numbers:

Superadiabatic (SA) techniques allow the engineering of adiabatic dynamics in finite time. While truly adiabatic transformations require infinitely slow driving, transitionless protocols may be implemented at finite speed by adding properly designed time-dependent terms $H_{SA}(t)$ to the Hamiltonian of a system [1, 2]. By suppressing nonadiabatic excitations, these fast processes reproduce the same final state as that of adiabatic driving. In that sense, they provide a shortcut to adiabaticity. In the last few years, there has been remarkable progress, both theoretical [1–7] and experimental [8–17], in developing superadiabatic methods for quantum and classical systems (see Ref. [18] for a review). Successful applications include high-fidelity driving of a BEC [11], fast transport of trapped ions [12, 13], fast adiabatic passage using a single spin in diamond [14] and cold atoms [15], as well as swift equilibration of a Brownian particle [16].

Superadiabatic protocols have recently been extended to thermal machines as a means to enhance their performance. Classical [19, 20] and quantum [21, 22] single particle heat engines, as well as multiparticle quantum motors [22–24] have been theoretically investigated. Nonadiabatic transitions are well-known sources of entropy production that reduce the efficiency of thermal machines [25–27]. Successfully suppressing them using superadiabatic methods thus appears a promising strategy to boost their work and power output.

However, a crucial point that needs to be addressed in order to assess the usefulness of shortcut techniques in thermodynamics is the proper computation of the efficiency of a superadiabatic engine. Since the excitation suppressing term $H_{SA}(t)$ in the Hamiltonian is often assumed to be zero at the begin and at the end of a transformation [18], its work contribution vanishes. The energetic cost of the additional superadiabatic driving is therefore commonly not included in the calculation of the efficiency [19–24]. As a result, the latter quantity reduces to the adiabatic efficiency, even for fast nonadiabatic driving of the machine: the superadiabatic driving thus appears to be for free. This situation is somewhat reminiscent of the power of a periodic signal which is zero at the beginning and at the end of one period. While the instantaneous power vanishes at the end of the interval, the actual power of the signal is given by the non-zero time-averaged power [28]. As a matter of

fact, the energetic cost of superadiabatic protocols was lately defined in universal quantum computation and adiabatic gate teleportation models as the time-averaged norm of the superadiabatic Hamiltonian $H_{SA}(t)$ [29, 30] (see also Refs. [31–34]). However, the chosen Hilbert-Schmidt norm is related to the variance of the energy and not to its mean [35]. It is hence of limited relevance to the investigation of the energetics of a heat engine.

In this paper, we evaluate the performance of a superadiabatic thermal machine by properly taking the energetic cost of the transitionless driving into account. We consider commonly employed local counterdiabatic (LCD) control techniques [5–7] which have latterly been successfully implemented experimentally in Refs. [9–11]. We evaluate both efficiency and power for a paradigmatic harmonic quantum Otto engine [36–41]. We explicitly compute the cost of the superadiabatic protocol as the time-averaged expectation value of the Hamiltonian $H_{SA}(t)$ for compression and expansion phases of the engine cycle. We find that the energetic cost of the superadiabatic driving exceeds the potential work gain for moderately rapid protocols. Superadiabatic engines may therefore only outperform traditional quantum motors for very fast cycles, albeit with an efficiency much smaller than the corresponding adiabatic efficiency. We additionally derive generic upper bounds on both superadiabatic efficiency and power, valid for any heat engine cycle, based on the concept of quantum speed limit times for driven unitary dynamics [42]. We demonstrate that these quantum bounds are tighter than conventional bounds that follow from the second law of thermodynamics.

Quantum Otto engine. We consider a quantum engine whose working medium is a harmonic oscillator with time-dependent frequency ω_t . The corresponding Hamiltonian is of the usual form, $H_0(t) = p^2/(2m) + m\omega_t^2 x^2/2$, where x and p are the position and momentum operators of an oscillator of mass m . The Otto cycle consists of four consecutive steps as shown in Fig. 1 [36–41]: (1) *Isentropic compression* $A \rightarrow B$: the frequency is varied from ω_1 to ω_2 during time τ_1 while the system is isolated. The evolution is unitary and the von Neumann entropy is constant. (2) *Hot isochore* $B \rightarrow C$: the oscillator is weakly coupled to a bath at inverse temperature β_2 at fixed frequency and thermalizes to state C during time τ_2 . (3) *Isentropic expansion* $C \rightarrow D$: the frequency is

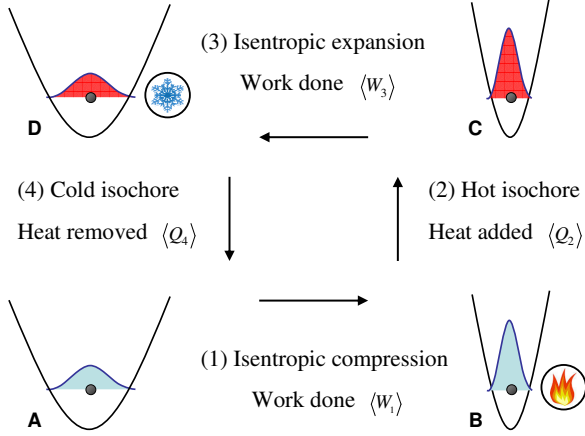


FIG. 1: Quantum Otto engine for a harmonic trap with time-dependent frequency. The cycle consists of four consecutive steps: (1) isentropic compression, (2) isochoric heating, (3) isentropic expansion and (4) isochoric cooling. Work is produced during the first and third unitary strokes, while heat is absorbed from the hot reservoir during the heating phase (2).

changed back to its initial value during time τ_3 at constant von Neumann entropy. (4) *Cold isochore* $D \rightarrow A$: the system is weakly coupled to a bath at inverse temperature $\beta_1 > \beta_2$ and relaxes to state A during τ_4 at fixed frequency. We will assume, as commonly done [36–41], that the thermalization times $\tau_{2,4}$ are much shorter than the compression/expansion times $\tau_{1,3}$. The total cycle time is then $\tau_{\text{cycle}} = \tau_1 + \tau_3 = 2\tau$ for equal step duration.

In order to evaluate the performance of the Otto engine, we need to compute work and heat for each of the above steps. Work is performed during the first and third unitary strokes, whereas heat is exchanged with the baths during the isochoric thermalization phases two and four. The mean work may be calculated by using the exact solution of the Schrödinger equation for the parametric oscillator for any given frequency modulation [43, 44]. For the compression/expansion steps, it is given by [41],

$$\langle W_1 \rangle = \frac{\hbar}{2} (\omega_2 Q_1^* - \omega_1) \coth \left(\frac{\beta_1 \hbar \omega_1}{2} \right), \quad (1)$$

$$\langle W_3 \rangle = \frac{\hbar}{2} (\omega_1 Q_3^* - \omega_2) \coth \left(\frac{\beta_2 \hbar \omega_2}{2} \right), \quad (2)$$

where we have introduced the dimensionless adiabaticity parameter Q_i^* ($i = 1, 3$) [45]. It is defined as the ratio of the mean energy and the corresponding adiabatic mean energy and is thus equal to one for adiabatic processes [44]. Its explicit expression for any frequency modulation ω_t may be found in Refs. [43, 44]. Furthermore, the mean

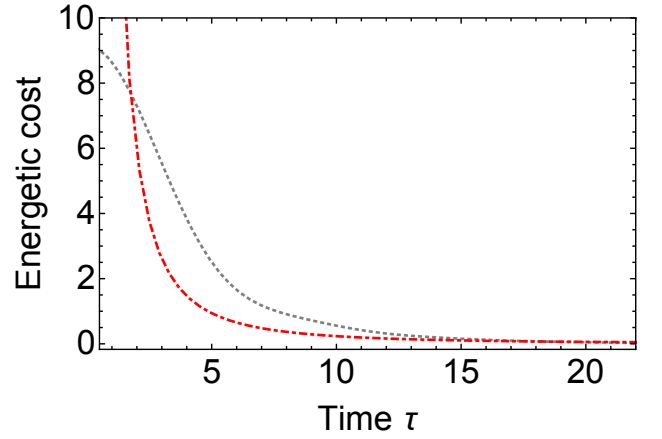


FIG. 2: Energetic cost of the superadiabatic driving $\langle H_{\text{SA}}^1 \rangle_\tau + \langle H_{\text{SA}}^3 \rangle_\tau$, each defined as the time average of Eq. (8), for the compression and expansion steps (1) and (3) (red dotted-dashed) as a function of the driving time τ . The corresponding nonadiabatic work $\langle W_1 \rangle_{\text{NA}} + \langle W_3 \rangle_{\text{NA}}$, defined as the difference between the actual and the adiabatic work, is shown for comparison (grey dotted). Parameters are $\omega_1 = 0.32$, $\omega_2 = 1$, $\beta_1 = 0.5$ and $\beta_2 = 0.05$.

heat absorbed from the hot bath reads [41],

$$\langle Q_2 \rangle = \frac{\hbar \omega_2}{2} \left[\coth \left(\frac{\beta_2 \hbar \omega_2}{2} \right) - Q_1^* \coth \left(\frac{\beta_1 \hbar \omega_1}{2} \right) \right]. \quad (3)$$

For an engine, the produced work is negative, $\langle W_1 \rangle + \langle W_3 \rangle < 0$, and the absorbed heat is positive, $\langle Q_2 \rangle > 0$.

Superadiabatic driving. The compression and expansion phases (1) and (3) may be sped up, while suppressing unwanted nonadiabatic transitions, by adding a local harmonic potential H_{SA} to the system Hamiltonian H_0 . The local counterdiabatic Hamiltonian may then written in the form $H_{\text{LCD}}(t) = H_0(t) + H_{\text{SA}}(t)$ with [5–7],

$$H_{\text{SA}} = \frac{m}{2} (\Omega_t^2 - \omega_t^2) x^2 = \frac{m}{2} \left(-\frac{3\dot{\omega}_t^2}{4\omega_t^2} + \frac{\ddot{\omega}_t}{2\omega_t} \right) x^2. \quad (4)$$

Boundary conditions ensuring that $H_{\text{SA}}(0, \tau) = 0$ at the beginning and at the end of the driving are given by,

$$\begin{aligned} \omega(0) &= \omega_i, & \dot{\omega}(0) &= 0, & \ddot{\omega}(0) &= 0, \\ \omega(\tau) &= \omega_f, & \dot{\omega}(\tau) &= 0, & \ddot{\omega}(\tau) &= 0, \end{aligned} \quad (5)$$

where $\omega_{i,f} = \omega_{1,2}$ denote the respective initial and final frequencies of the compression/expansion steps. The conditions (5) are, for instance, satisfied by [5–7],

$$\omega_t = \omega_i + 10(\omega_f - \omega_i)s^3 - 15(\omega_f - \omega_i)s^4 + 6(\omega_f - \omega_i)s^5, \quad (6)$$

with $s = t/\tau$. Note that $\Omega_t^2 > 0$ to avoid trap inversion. Implementing the superadiabatic driving (4) leads to a unit adiabaticity parameter, $Q_i^*(\tau) = 1$ ($i = 1, 3$). As a consequence, the work performed in finite time during the two compression/expansion phases is equal to the adiabatic work, $\langle W_1 \rangle_{\text{SA}} = \langle W_1 \rangle_{\text{AD}}$ and $\langle W_3 \rangle_{\text{SA}} = \langle W_3 \rangle_{\text{AD}}$.

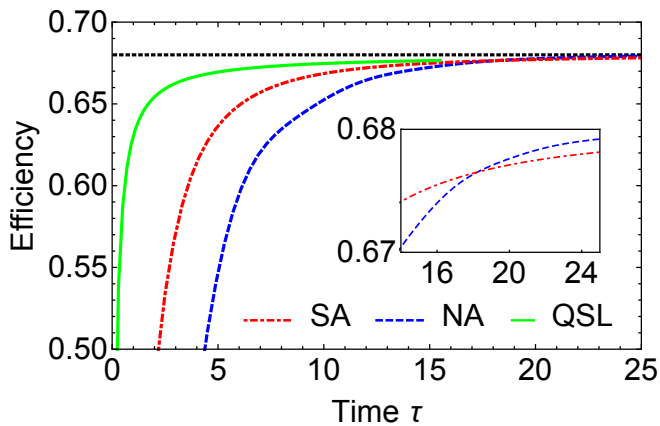


FIG. 3: Superadiabatic efficiency η_{SA} (red dotted-dashed), Eq. (7), together with the nonadiabatic efficiency η_{NA} (blue dashed) and the adiabatic efficiency η_{AD} (black dotted) as a function of the time τ . The green solid line shows the quantum speed limit bound (11). Same parameters as in Fig. 2.

Efficiency of the superadiabatic engine. We define the efficiency of the superadiabatic motor as,

$$\eta_{SA} = \frac{\text{energy output}}{\text{energy input}} = \frac{-\langle W_1 \rangle_{SA} + \langle W_3 \rangle_{SA}}{\langle Q_2 \rangle + \langle H_{SA}^1 \rangle_\tau + \langle H_{SA}^3 \rangle_\tau}. \quad (7)$$

In the above expression, the energetic cost of the transitionless driving is taken into account by including the time-average, $\langle H_{SA}^i \rangle_\tau = (1/\tau) \int_0^\tau dt \langle H_{SA}^i(t) \rangle$ ($i = 1, 3$), of the local potential (4) for the compression/expansion steps. Equation (7) reduces to the adiabatic efficiency η_{AD} in the absence of these two contributions. For further reference, we also introduce the usual nonadiabatic efficiency of the engine, $\eta_{NA} = -(\langle W_1 \rangle + \langle W_3 \rangle) / \langle Q_2 \rangle$, based on the formulas (1)-(3) without any shortcut.

The expectation value of the local counterdiabatic potential (4) may be calculated explicitly for an initial thermal state in terms of the initial energy of the system $\langle H_0(0) \rangle$. We find (see Supplemental Material [46]),

$$\langle H_{SA}(t) \rangle = \frac{\omega_t}{\omega_i} \langle H_0(0) \rangle \left[-\frac{\dot{\omega}_t^2}{4\omega_t^4} + \frac{\ddot{\omega}_t}{4\omega_t^3} \right]. \quad (8)$$

We use Eq. (8) to numerically compute the time averages $\langle H_{SA}^i \rangle_\tau$ ($i = 1, 3$) for compression/expansion that are needed to evaluate the superadiabatic efficiency (7).

Figure 2 shows, as an illustration, the energetic cost of the superadiabatic driving $\langle H_{SA}^1 \rangle_\tau + \langle H_{SA}^3 \rangle_\tau$, for the compression and expansion steps (1) and (3) as a function of the driving time τ . We also display, for comparison, the corresponding nonadiabatic work $\langle W_1 \rangle_{NA} + \langle W_3 \rangle_{NA}$, defined as the difference between the actual work and the adiabatic work, $\langle W_i \rangle_{NA} = \langle W_i \rangle - \langle W_i \rangle_{AD}$ ($i = 1, 3$); this quantity measures the importance of nonadiabatic excitations induced by fast protocols and is often referred to as internal friction [21, 27, 31, 39]. We observe that the

time-averaged superadiabatic energy (red dotted-dashed) increases significantly with decreasing process time as expected. This increase is much faster than that of the nonadiabatic work $\langle W_1 \rangle_{NA} + \langle W_3 \rangle_{NA}$ (grey dotted). Eventually, for very rapid driving, the energetic price of the shortcut will dominate nonadiabatic energy losses.

Figure 3 exhibits the superadiabatic efficiency η_{SA} (red dotted-dashed), Eq. (7), as a function of the driving time τ , together with the adiabatic efficiency η_{AD} (black dotted) and the nonadiabatic efficiency η_{NA} (blue dashed). Three points are worth emphasizing: i) if the energetic cost of the shortcut is not included, the superadiabatic efficiency is equal to the maximum possible value given by the constant adiabatic efficiency η_{AD} , as noted in Refs. [19–24], ii) by contrast, if that energetic cost is properly taken into account, the superadiabatic efficiency η_{SA} drops for decreasing τ , reflecting the sharp augmentation of the time-averaged superadiabatic energy seen in Fig. 2, iii) we further observe that $\eta_{SA} < \eta_{NA}$ for large time τ , while $\eta_{SA} > \eta_{NA}$ only for small enough τ (inset). We can thus conclude that the superadiabatic driving is only of advantage for sufficiently short cycle durations. For large cycle times, the energetic cost of the shortcut outweighs the work gained by emulating adiabaticity.

Another benefit of the superadiabatic driving appears for very small time τ . An examination of Eq. (3) reveals that the heat $\langle Q_2 \rangle$ becomes negative for very strongly nonadiabatic processes, when $Q_1^*(\tau) > \coth(\beta_2 \hbar \omega_2 / 2) / \coth(\beta_1 \hbar \omega_1 / 2)$. In this regime, heat is pumped into the hot reservoir, instead of being absorbed from it, and the machine stops working as an engine [47]. Since $Q_1^*(\tau) = 1$ for all τ for the local counterdiabatic driving, this problem never occurs for the superadiabatic motor, even in the limit of very short cycles $\tau \rightarrow 0$.

Power of the superadiabatic engine. The power of the superadiabatic machine is given by,

$$P_{SA} = -\frac{\langle W_1 \rangle_{SA} + \langle W_3 \rangle_{SA}}{\tau_{\text{cycle}}}. \quad (9)$$

Since the superadiabatic protocol ensures adiabatic work output, $\langle W_i \rangle_{SA} = \langle W_i \rangle_{AD}$ ($i = 1, 3$), in a shorter cycle duration τ_{cycle} , the superadiabatic power P_{SA} is always greater than the nonadiabatic power $P_{NA} = -(\langle W_1 \rangle + \langle W_3 \rangle) / \tau_{\text{cycle}}$ (see Fig. 4). This ability to considerably enhance the power of a thermal machine is one of the true advantages of the shortcut to adiabaticity approach. However, in view of the discussion above, it is not possible to reach arbitrarily large power at maximum efficiency, as sometimes claimed [19–22]. This observation is in complete agreement with recent general proofs that forbid the simultaneous attainability of maximum power and maximum efficiency [48].

Universal quantum speed limit bounds. We finally derive generic upper bounds for both the superadiabatic efficiency (7) and the superadiabatic power (9), based on the concept of quantum speed limits (see Refs. [49–51] and references therein). Contrary to classical physics, quantum theory limits the speed of evolution of a system

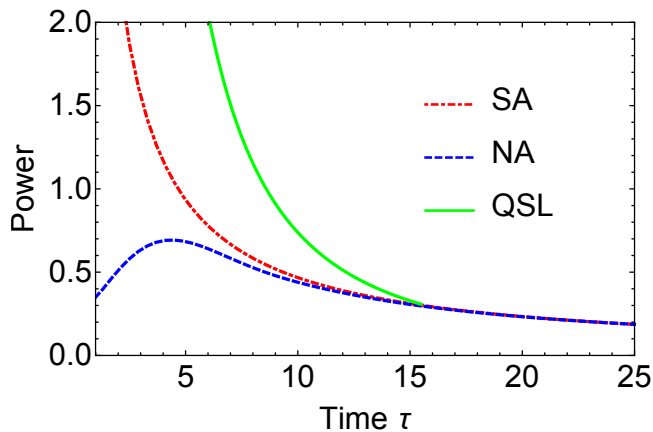


FIG. 4: Superadiabatic power P_{SA} (red dotted-dashed), Eq. (8), together with the nonadiabatic power P_{NA} (blue dashed) as a function of the driving time τ . The green solid line shows the quantum speed limit bound (12). Same parameters as in Fig. 2.

between given initial and final states. In particular, there exists a lower bound, called the quantum speed limit time $\tau_{QSL} \leq \tau$, on the time a system needs to evolve between these two states. An important restriction of the superadiabatic technique is the time required to successfully implement the counterdiabatic driving (4), which depends on the first two time derivatives of the frequency ω_t [52]. For this unitary driven dynamics, a Margolus-Levitin-type bound on the evolution time reads [42],

$$\tau \geq \tau_{QSL} = \frac{\hbar \mathcal{L}(\rho_i, \rho_f)}{\langle H_{SA} \rangle_\tau}, \quad (10)$$

where $\mathcal{L}(\rho_i, \rho_f)$ denotes the Bures angle between the initial and final density operators of the system [46, 53] and $\langle H_{SA} \rangle_\tau$ the time-averaged superadiabatic energy (8). We expect Eq. (10) to be a proper bound for the compression/expansion phases, when the engine dynamics is dominated by the superadiabatic driving for small τ .

To derive an upper bound on the superadiabatic efficiency (7), we use inequality (10) to obtain,

$$\eta_{SA} \leq \eta_{SA}^{QSL} = -\frac{\langle W_1 \rangle_{AD} + \langle W_3 \rangle_{AD}}{\langle Q_2 \rangle + \hbar(\mathcal{L}_1 + \mathcal{L}_3)/\tau}, \quad (11)$$

where \mathcal{L}_i ($i = 1, 3$) are the respective Bures angles for the compression/expansion steps. On the other hand, an upper bound on the superadiabatic power (9) is,

$$P_{SA} \leq P_{SA}^{QSL} = -\frac{\langle W_1 \rangle_{AD} + \langle W_3 \rangle_{AD}}{\tau_{QSL}^1 + \tau_{QSL}^3}, \quad (12)$$

where τ_{QSL}^i ($i = 1, 3$) are the respective speed-limit bounds (10) for the compression/expansion phases.

The two quantum speed limit bounds (11) and (12) are shown in Figs. (3)-(4) (green solid). We first notice that

the quantum bound (11) on the efficiency is sharper than the thermodynamic bound given by the constant adiabatic efficiency η_{AD} . Remarkably, quantum theory further imposes an upper bound on the power, whereas the second law of thermodynamics does not [48]. Quantum thermodynamics hence establishes tighter bounds than classical thermodynamics. The latter result may be understood by noting that thermodynamics does not have the notion of time scale, contrary to quantum mechanics. Finally, we stress that the two speed limit bounds directly follow from the definitions of efficiency and power. As a result, they are independent of the thermodynamic cycle considered and generically apply to any quantum heat engine, not just to the quantum Otto motor.

Conclusions. We have performed a detailed study of both efficiency and power of a superadiabatic quantum heat engine. We have explicitly accounted for the energetic cost of the superadiabatic driving, defined as the time average of the local counterdiabatic potential. We have found that the efficiency of the engine markedly drops with decreasing cycle time. However, this drop is much slower than that of the nonadiabatic efficiency without the shortcut. As result, superadiabatic machines outperforms their conventional counterparts for very short cycles, when the work gain generated by the counterdiabatic driving outweighs its energetic cost. We have additionally derived generic upper bound on superadiabatic efficiency and power based on the idea of quantum speed limits. These quantum bounds, valid for general thermal motors, are tighter than the usual bounds based on the second law of thermodynamics. We therefore expect them to be useful for future investigations of thermal machines in the quantum regime.

Acknowledgments This work was partially supported by the EU Collaborative Project TherMiQ (Grant Agreement 618074) and the COST Action MP1209.

Supplemental Material

Appendix A: Local counterdiabatic energy

We here present a derivation of the mean energy of the local counterdiabatic Hamiltonian H_{LCD} and of the corresponding adiabaticity parameter Q_{LCD}^* used during the compression/expansion protocols. We consider a time-dependent harmonic oscillator with Hamiltonian,

$$H_0(t) = \frac{p^2}{2m} + \frac{m\omega_t^2 x^2}{2}, \quad (A1)$$

where ω_t is the time-dependent angular frequency, m the mass, and (p, x) the respective momentum and position operators. The initial energy eigenstates at $t = 0$ with $\omega(0) = \omega_0$ in coordinate representation are given by

$$\psi_n(x, 0) = \frac{1}{\sqrt{2^n n!}} \left(\frac{m\omega_0}{\pi \hbar} \right)^{1/4} \exp\left(-\frac{m\omega_0}{2\hbar} x^2\right) \mathcal{H}_n\left(\sqrt{\frac{m\omega_0}{\hbar}} x\right), \quad (A2)$$

where \mathcal{H}_n are Hermite polynomials and $E_n^0 = \hbar\omega_0(n + 1/2)$ the corresponding energy eigenvalues. The instantaneous eigenstates and their corresponding eigenvalues are obtained by replacing ω_0 with ω_t .

The shortcut to adiabaticity may be implemented by adding a time-dependent counterdiabatic (CD) term to the system Hamiltonian (A1) [3–6]:

$$H_{\text{SA}}^{\text{CD}}(t) = -\frac{\dot{\omega}_t}{4\omega_t}(xp + px) = i\hbar\frac{\dot{\omega}_t}{4\omega_t}(a^2 - a^{\dagger 2}). \quad (\text{A3})$$

The last equality is obtained by expressing $x = \sqrt{\hbar/2m\omega_t}(a^\dagger + a)$ and $p = i\sqrt{\hbar m\omega_t}/2(a^\dagger - a)$, in terms of the annihilation and creation operators a and a^\dagger . The total Hamiltonian $H_{\text{CD}}(t) = H_0(t) + H_{\text{SA}}^{\text{CD}}(t)$ is still quadratic in x and p and may thus be considered that of a generalized harmonic oscillator [4, 54]. However, since the Hamiltonian (A3) is a nonlocal operator, it is often convenient to look for a unitarily equivalent Hamiltonian with a local potential [5, 6]. Applying the canonical transformation, $U_x = \exp(im\dot{\omega}x^2/4\hbar\omega)$, which cancels the cross terms xp and px , to the Hamiltonian (A3) leads to a new local counterdiabatic (LCD) Hamiltonian of the form [5, 6],

$$\begin{aligned} H_{\text{LCD}}(t) &= U_x^\dagger(H_{\text{CD}}(t) - i\hbar\dot{U}_x U_x^\dagger)U_x \\ &= \frac{p^2}{2m} + \frac{m\Omega_t^2 x^2}{2}, \end{aligned} \quad (\text{A4})$$

with the modified time-dependent (squared) frequency,

$$\Omega^2(t) = \omega_t^2 - \frac{3\dot{\omega}_t^2}{4\omega_t^2} + \frac{\ddot{\omega}_t}{2\omega_t}. \quad (\text{A5})$$

This resulting Hamiltonian is local and still drives the evolution along the adiabatic trajectory of the system of interest. By demanding that $H_{\text{LCD}} = H_0$ at $t = 0, \tau$ and imposing $\dot{\omega}(\tau) = \ddot{\omega}(\tau) = 0$, the final state is equal for

both dynamics, even in phase, and the final vibrational state populations coincide with those of a slow adiabatic process [5]. It can be readily shown that $\Omega^2(t)$ approaches $\omega^2(t)$ for very slow expansion/compression process [6].

Exact solutions of the Schrödinger equation for a time-dependent harmonic oscillator have been extensively investigated [55–57]. Following Lohe [57], a solution based on the invariants of motion is of the form,

$$I(t) = \frac{b^2}{2m}p^2 + \frac{mb^2}{2}x^2 - \frac{b\dot{b}}{2}(px + xp) + \frac{m\omega_0^2}{2b^2}x^2, \quad (\text{A6})$$

where ω_0 is an arbitrary constant—a convenient choice is to set $\omega_0 = \omega(0)$, ($\omega_0^2 > 0$). The scaling factor $b = b(t)$ is a solution of the Ermakov differential equation,

$$\ddot{b} + \omega_t^2 b = \omega_0^2/b^3. \quad (\text{A7})$$

In the adiabatic limit, $\ddot{b} \simeq 0$ and

$$b(t) \rightarrow b_{\text{ad}} = \sqrt{\frac{\omega_0}{\omega_t}}. \quad (\text{A8})$$

Equation (A7) is valid for any given ω_t and its general solution can be constructed from the solutions $f(t)$ of the linear equation of motion for the classical time-dependent harmonic oscillator [58],

$$\ddot{f} + \omega_t^2 f = 0, \quad (\text{A9})$$

according to $b^2/\omega_0 = f_1^2 + W^{-2}f_2^2$, where f_1, f_2 are independent solutions of Eq. (A9) and the Wronskian $W[f_1, f_2] = f_1\dot{f}_2 - \dot{f}_1f_2$ is a nonzero constant. We note that the Wronskian properties of Eq. (A9) can be used to show the equivalence of the adiabaticity parameter derived here and that of Husimi [44, 45] (see Ref. [23]). The general solution of the time-dependent Schrödinger equation for the Hamiltonian (A4) is hence,

$$\Psi_n(x, t) = \frac{1}{\sqrt{2^n n!}} \left(\frac{m\omega_0}{\pi\hbar b^2}\right)^{1/4} \exp\left[\frac{im\dot{b}}{2\hbar b}x^2 - i\int_0^t \frac{\omega_0(n+1/2)}{b(t')^2} dt'\right] \exp\left(-\frac{m\omega_0}{2\hbar b^2}x^2\right) \mathcal{H}_n\left(\sqrt{\frac{m\omega_0}{\hbar}}\frac{x}{b}\right). \quad (\text{A10})$$

The time-dependent energy eigenstates, $H_{\text{LCD}}|\Psi_n(x, t)\rangle = E|\Psi_n(x, t)\rangle$, are explicitly given by,

$$\begin{aligned} E &= \langle\Psi_n(x, t)|H_{\text{LCD}}|\Psi_n(x, t)\rangle \\ &= \frac{E_n^0}{b^2} - \frac{m}{2}(b\ddot{b} - \dot{b}^2)\langle\Psi_n(x, 0)|x^2|\Psi_n(x, 0)\rangle \\ &\quad + \frac{\dot{b}}{2b}\langle\Psi_n(x, 0)|xp + px|\Psi_n(x, 0)\rangle. \end{aligned} \quad (\text{A11})$$

We next consider a quantum oscillator initially pre-

pared in thermal equilibrium state with density operator,

$$\rho_{\text{eq}} = \sum_{n=0}^{\infty} p_n^0 |\Psi_n(x, 0)\rangle\langle\Psi_n(x, 0)|, \quad (\text{A12})$$

where $p_n^0 = \exp(-\beta E_n^0)/Z_0$ is the probability that the oscillator is in state $|\Psi_n(x, 0)\rangle$ and Z_0 is the partition function. The initial thermal mean energy at $t = 0$ is accordingly,

$$\langle H(0) \rangle = m\omega_0^2 \langle x^2(0) \rangle = \frac{\hbar\omega_0}{2} \coth\left(\frac{\beta\hbar\omega_0}{2}\right). \quad (\text{A13})$$

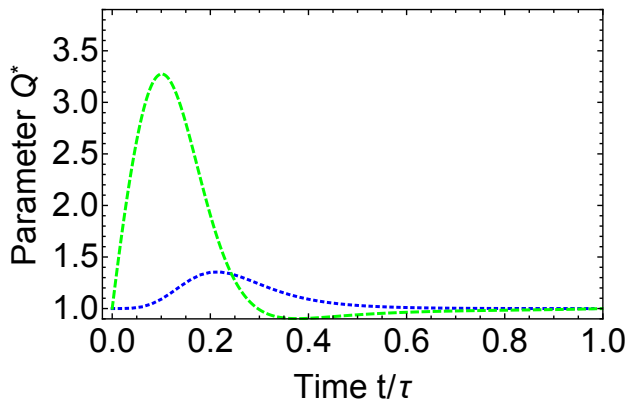


FIG. 5: Adiabaticity parameter $Q_{\text{LCD}}^*(t)$, Eq. (18), (green dashed) and Eq. (51) of Ref. [22], $\bar{Q}_{\text{LCD}}^*(t) = 1 + \dot{\omega}_t^2/(8\omega_t^4)$, (blue dotted) as a function of t/τ for $\omega_0/\omega_1 = 0.15$.

The expectation value of the local counterdiabatic Hamiltonian $H_{\text{LCD}}(t)$ at time t follows from Eqs. (11)-(13) as

$$\begin{aligned} \langle H_{\text{LCD}}(t) \rangle &= \sum_{n=0}^{\infty} p_n^0 \langle \Psi_n(x, t) | H_{\text{LCD}} | \Psi_n(x, t) \rangle \\ &= \frac{\langle H(0) \rangle}{b^2} + \frac{(b\ddot{b} - b\dot{b})}{2\omega_0^2} \langle H(0) \rangle, \end{aligned} \quad (\text{A14})$$

where we have used the fact that $\langle \{x, p\}(0) \rangle = 0$ for thermal equilibrium state. Since the squared frequency (A5) can be rewritten in the adiabatic limit as,

$$\Omega_t^2 = \omega_t^2 - \frac{\ddot{b}_{ad}}{b_{ad}}, \quad (\text{A15})$$

we obtain, using Eqs. (A5), (A8) and (A15), the expression,

$$b\ddot{b} - b\dot{b} = b_{ad}^2 \left\{ -\frac{\ddot{\omega}_t}{2\omega_t} + \frac{1}{2} \left(\frac{\dot{\omega}_t}{\omega_t} \right)^2 \right\}. \quad (\text{A16})$$

$$\mathcal{F}(\rho_\tau, \rho_0) = \frac{2}{\sqrt{ct^2(\beta\epsilon_0/2) + ct^2(\beta\epsilon_1/2) + 2Q^*ct(\beta\epsilon_0/2)ct(\beta\epsilon_1/2) + c^2(\beta\epsilon_0/2)c^2(\beta\epsilon_1/2) - c(\beta\epsilon_0/2)c(\beta\epsilon_1/2)}}. \quad (\text{C1})$$

where $\epsilon_i = \hbar\omega_i$, $ct(x) = \coth(x)$ and $c(x) = \text{csch}(x)$.

Finally, substituting Eq. (A16) into Eq. (A14), the mean energy of the local counterdiabatic driving is found to be,

$$\langle H_{\text{LCD}}(t) \rangle = \frac{Q_{\text{LCD}}^*(t)}{b_{ad}^2} \langle H(0) \rangle, \quad (\text{A17})$$

where the adiabaticity parameter $Q_{\text{LCD}}^*(t)$ is given by,

$$Q_{\text{LCD}}^*(t) = 1 - \frac{\dot{\omega}_t^2}{4\omega_t^4} + \frac{\ddot{\omega}_t}{4\omega_t^3}. \quad (\text{A18})$$

Note that Eq. (A18) corrects Eq. (51) in Ref. [22].

Appendix B: Superadiabatic energy

The expectation value of the superadiabatic potential H_{SA} may be evaluated from Eqs. (4) and (17). We have,

$$\begin{aligned} H_{\text{SA}}(t) &= H_{\text{LCD}}(t) - H_0(t) \\ &= \frac{m}{2} \left(-\frac{3\dot{\omega}_t^2}{4\omega_t^2} + \frac{\ddot{\omega}_t}{2\omega_t} \right) x^2. \end{aligned} \quad (\text{B1})$$

As a consequence, we obtain,

$$\langle H_{\text{SA}}(t) \rangle = \frac{\omega_t}{\omega_0} \langle H(0) \rangle \left[-\frac{\dot{\omega}_t^2}{4\omega_t^4} + \frac{\ddot{\omega}_t}{4\omega_t^3} \right]. \quad (\text{B2})$$

The properties of the shortcut imply that $\langle H_{\text{SA}}(0, \tau) \rangle = 0$ at the beginning and at the end of the protocol.

Appendix C: Bures length

The Bures length between initial and final density operators of the system is $\mathcal{L}(\rho_\tau, \rho_0) = \arccos \sqrt{F(\rho_\tau, \rho_0)}$, where the $F(\rho_\tau, \rho_0)$ is the fidelity between the two states [59]. For the considered driven harmonic oscillator, initial and final states are Gaussian and the fidelity is explicitly given by [53]:

-
- [1] M. Demirplak and S.A. Rice, Adiabatic population transfer with control fields, *J. Phys. Chem. A* **107**, 9937 (2003).
 [2] M.V. Berry, Transitionless quantum driving, *J. Phys. A* **42**, 365303 (2009).

- [3] J.G. Muga, X. Chen, S. Ibáñez, I. Lizuain, and A. Ruschhaupt, Transitionless quantum drivings for the harmonic oscillator, *J. Phys. B* **43**, 085509 (2010).
 [4] X. Chen, A. Ruschhaupt, S. Schmidt, S. Ibáñez, and J.G. Muga, Shortcut to adiabaticity in harmonic traps, *J. At.*

- Mol. Sci. **1**, 1 (2010).
- [5] S. Ibáñez, X. Chen, E. Torrontegui, J.G. Muga and A. Ruschhaupt, Multiple Schrödinger Pictures and Dynamics in Shortcuts to Adiabaticity, *Phys. Rev. Lett.* **109**, 100403 (2012).
 - [6] A. del Campo, Shortcuts to Adiabaticity by Counterdiabatic Driving, *Phys. Rev. Lett.* **111**, 100502 (2013).
 - [7] S. Deffner, C. Jarzynski, and A. del Campo, Classical and quantum shortcuts to adiabaticity for scale-invariant driving, *Phys. Rev. X* **4**, 021013 (2014).
 - [8] A. Couvert, T. Kawalec, G. Reinaudi, and D. Guery-Odelin, Optimal transport of ultracold atoms in the non-adiabatic regime, *EPL* **83**, 13001 (2008).
 - [9] J.-F. Schaff, X.-L. Song, P. Vignolo and G. Labeyrie, Fast optimal transition between two equilibrium states, *Phys. Rev. A* **82**, 033430 (2010).
 - [10] J.-F. Schaff, X.-L. Song, P. Capuzzi, P. Vignolo, and G. Labeyrie, Shortcut to adiabaticity for an interacting Bose-Einstein condensate, *EPL* **93**, 23001 (2011).
 - [11] M. G. Bason, M. Viteau, N. Malossi, P. Huillery, E. Arimondo, D. Ciampini, R. Fazio, V. Giovannetti, R. Mannella, and O. Morsch, High-fidelity quantum driving, *Nat. Phys.* **8**, 147 (2012).
 - [12] R. Bowler, J. Gaebler, Y. Lin, T. Tan, D. Hanneke, J. Jost, J. Home, D. Leibfried, and D. Wineland, Coherent diabatic ion transport and separation in a multizone trap array, *Phys. Rev. Lett.* **109** 080502 (2012).
 - [13] A. Walther, F. Ziesel, T. Ruster, S. T. Dawkins, K. Ott, M. Hettrich, K. Singer, F. Schmidt-Kaler, and U. Poschinger, Controlling Fast Transport of Cold Trapped Ions, *Phys. Rev. Lett.* **109**, 080501 (2012).
 - [14] J. Zhang, J. Hyun Shim, I. Niemeyer, T. Taniguchi, T. Teraji, H. Abe, S. Onoda, T. Yamamoto, T. Ohshima, J. Isoya, and D. Suter, Experimental Implementation of Assisted Quantum Adiabatic Passage in a Single Spin, *Phys. Rev. Lett.* **110**, 240501 (2013).
 - [15] Y-X. Du, Z-T. Liang, Y-C. Li, X-X. Yue, Q-X. Lv, W. Huang, X. Chen, H. Yan and S-L. Zhu, Experimental realization of stimulated Raman shortcut-to-adiabatic passage with cold atoms, *Nat. Comm.* **7**, 12479 (2016).
 - [16] I. Martinez, A. Petrosyan, D. Guery-Odelin, E. Trizac, S. Ciliberto, Engineered swift equilibration of a Brownian particle, *Nature Phys.* **12**, 843 (2016).
 - [17] S. An, D. Lv, A. del Campo, and K. Kim, Shortcuts to Adiabaticity by Counterdiabatic Driving in Trapped-ion Transport, *Nature Comm.* (2016).
 - [18] E. Torrontegui et al, *Chapter 2. Shortcuts to adiabaticity*, *Adv. At. Mol. Opt. Phys.* **62**, 117 (2013).
 - [19] J. Deng, Q.-h. Wang, Z. Liu, P. Hänggi, and J. Gong, Boosting work characteristics and overall heat-engine performance via shortcuts to adiabaticity: Quantum and classical systems, *Phys. Rev. E* **88**, 062122 (2013).
 - [20] Z. C. Tu, Stochastic heat engine with the consideration of inertial effects and shortcuts to adiabaticity, *Phys. Rev. E* **89**, 052148 (2014).
 - [21] A. del Campo, J. Goold, and M. Paternostro, More bang for your buck: Super-adiabatic quantum engines, *Sci. Rep.* **4**, 6208 (2014).
 - [22] M. Beau, J. Jaramillo, and A. del Campo, Scaling-Up Quantum Heat Engines Efficiently via Shortcuts to Adiabaticity, *Entropy* **18**, 168 (2016).
 - [23] J. Jaramillo, M. Beau, and A. del Campo, Quantum Supremacy of Many-Particle Thermal Machines, *New. J. Phys.* **18**, 075019 (2016).
 - [24] L. Chotorlishvili, M. Azimi, S. Stagraczynski, Z. Toklikishvili, M. Schüler, and J. Berakdar, Superadiabatic quantum heat engine with a multiferroic working medium, *Phys. Rev. E* **94**, 032116 (2016).
 - [25] B. Andresen, P. Salamon, and R. S. Berry, Thermodynamics in Finite Time, *Phys. Today* **37**, 62 (1984).
 - [26] B. Andresen, Current Trends in Finite-Time Thermodynamics, *Angew. Chem. Int. Ed.* **50**, 2690 (2011).
 - [27] T. Feldmann and R. Kosloff, Performance of Discrete Heat Engines and Heat Pumps in Finite Time, *Phys. Rev. E* **61**, 4774 (2000).
 - [28] D. Haliday, R. Resnick and J. Walker, *Fundamentals of Physics* (Wiley, New York, 2013).
 - [29] A. C. Santos and M. S. Sarandy, Superadiabatic Controlled Evolutions and Universal Quantum Computation, *Sci. Rep.* **5**, 15775 (2015).
 - [30] A. C. Santos, R. D. Silva, and M. S. Sarandy, Shortcut to adiabatic gate teleportation, *Phys. Rev. A* **93**, 012311 (2016).
 - [31] Y. Zheng, S. Campbell, G. De Chiara, and D. Poletti, Cost of counterdiabatic driving and work output, *Phys. Rev. A* **94**, 042132 (2016).
 - [32] I. B. Coulamy, A. C. Santos, I. Hen, and M. S. Sarandy, Energetic cost of superadiabatic quantum computation, arXiv:1603.07778.
 - [33] S. Campbell and S. Deffner, Trade-off between speed and cost in shortcuts to adiabaticity, arXiv:1609.04662.
 - [34] K. Funo, J.-N. Zhang, C. Chatou, K. Kim, M. Ueda and A. del Campo, Universal Work Fluctuations during Shortcuts To Adiabaticity by Counterdiabatic Driving, arXiv:1609.08889
 - [35] S. Deffner and E. Lutz, Quantum speed limit for non-Markovian dynamics, *Phys. Rev. Lett.* **111**, 010402 (2013).
 - [36] R. Kosloff, A Quantum Mechanical Open System as a Model of a Heat Engine, *J. Chem. Phys.* **80**, 1625 (1984).
 - [37] E. Geva and R. Kosloff, On the Classical Limit of Quantum Thermodynamics in Finite Time, *J. Chem. Phys.* **96**, 3054 (1992).
 - [38] B. Lin and J. Chen, Performance analysis of an irreversible quantum heat engine working with harmonic oscillators, *Phys. Rev. E* **67**, 046105 (2003).
 - [39] Y. Rezek and R. Kosloff, Irreversible performance of a quantum harmonic heat engine, *New. J. Phys.* **8**, 83 (2006).
 - [40] H. T. Quan, Y. Liu, C. P. Sun, and F. Nori, Quantum thermodynamic cycles and quantum heat engines *Phys. Rev. E* **76**, 031105 (2007).
 - [41] O. Abah, J. Rossnagel, G. Jakob, S. Deffner, F. Schmidt-Kaler, K. Singer, and E. Lutz, Single-ion heat engine at maximum power, *Phys. Rev. Lett.* **112**, 030602 (2012).
 - [42] S. Deffner and E. Lutz, Energy-time uncertainty relation for driven quantum systems, *J. Phys. A* **46**, 335302 (2013).
 - [43] S. Deffner and E. Lutz, Nonequilibrium work distribution of a quantum harmonic oscillator, *Phys. Rev. E* **77**, 021128 (2008).
 - [44] S. Deffner, O. Abah, and E. Lutz, Quantum work statistics of linear and nonlinear parametric oscillators, *Chem. Phys.* **375**, 200 (2010).
 - [45] K. Husimi, *Miscellanea in elementary quantum mechanics*, *Prog. Theor. Phys.* **9**, 381 (1953).
 - [46] See Supplemental Material.
 - [47] O. Abah and E. Lutz, Optimal performance of a quantum

- Otto refrigerator, EPL **113**, 60002 (2016).
- [48] N. Shiraishi, K. Saito, and H. Tasaki, Universal Trade-Off Relation between Power and Efficiency for Heat Engines, Phys. Rev. Lett. **117**, 190601 (2016).
- [49] J. Anandan and Y. Aharonov, Geometry of Quantum Evolution, Phys. Rev. Lett. **65**, 1697 (1990).
- [50] L. Vaidman, Minimum time for the evolution to an orthogonal quantum state, Am. J. Phys. **60**, 182 (1991).
- [51] J. Uffink, The rate of evolution of a quantum state, Am. J. Phys. **61**, 935 (1993).
- [52] In cases where the system Hamiltonian H_0 limits the evolution speed, the superadiabatic approach will only have a restricted applicability.
- [53] S. Deffner and E. Lutz, Thermodynamic length for far-from-equilibrium quantum systems, Phys. Rev. E **87**, 022143 (2013).
- [54] M.V. Berry, Classical adiabatic angles and quantal adiabatic phase, J. Phys. A: Math. Gen. **18**, 15 (1985).
- [55] H. R. Lewis and W. B. Riesenfeld, An Exact Quantum Theory of the Time-Dependent Harmonic Oscillator and of a Charged Particle in a Time-Dependent Electromagnetic Field, J. Math. Phys. **10**, 1458 (1969).
- [56] M.V. Berry and G. Klein, Newtonian trajectories and quantum waves in expanding force fields, J. Phys. A **17**, 1805 (1984).
- [57] M. A. Lohe, Exact time dependence of solutions to the time-dependent Schrödinger equation, J. Phys. A: Math. Gen. **42**, 035307 (2009).
- [58] E. Pinney, The nonlinear differential equation $y'' + p(x)y + cy^{-3} = 0$, Proc. Amer. Math. Soc. **1**, 681 (1950).
- [59] H. Scutaru, Fidelity for displaced squeezed thermal states and the oscillator semigroup, J. Phys. A: Math. Gen. **31**, 3659 (1998).